

Identification of Active Crystalline Phase in La-K-Cu-V Mixed Oxide for the Simultaneous Removal of Nitrogen Oxides and Diesel Soot

Yasutake Teraoka,* Wengfeng Shangguan,† Kjell Jansson,†† Mats Nygren,†† and Shuichi Kagawa

Department of Applied Chemistry, Faculty of Engineering, Nagasaki University, Nagasaki 852-8521

†Department of Marine Resources Research and Development, Graduate School of Marine Science and Engineering, Nagasaki University, Nagasaki 852-8521

††Department of Inorganic Chemistry, Arrhenius Laboratory, Stockholm University, S-10691 Stockholm, Sweden

(Received June 29, 1998)

The oxide catalyst having an overall metal composition of La/K/Cu/V = 9/1/7/3 (denoted as LKCVO) showed an excellent selectivity to NO_x reduction into N₂ in the simultaneous NO_x-soot removal reaction, though it was a mixture of several crystalline phases. In order to identify the real active phase, LKCVO was characterized by X-ray diffraction (XRD) and by elemental analysis of individual grains in a transmission electron microscope (TEM) equipped with an energy dispersive spectrometer (EDS). LKCVO was found to be composed of CuO and mixed metal oxides analogous to La₂CuO₄, LaVO₄, and La₃VO₇. By comparing the catalytic activity of LKCVO with those of single-phase oxides synthesized according to the results of XRD and TEM/EDS, (La_{2-x}K_x)(Cu_{0.95}V_{0.05})O₄ with 0.05 ≤ x ≤ 0.1 was identified to be the real active phase in LKCVO for the simultaneous NO_x-soot removal reaction.

The catalytic reduction of nitrogen oxides (NO_x) into N₂ by the Diesel soot in an oxidizing atmosphere, which was first reported by Yoshida et al. in 1989,¹⁾ is a desirable after-treatment process of Diesel exhausts.²⁾ This reaction is designated the simultaneous removal of NO_x and soot, because harmful NO_x and soot can be removed simultaneously from the Diesel exhausts. So far, promoted CuO,¹⁾ perovskite-type oxide,^{3,4)} K₂NiF₄-type oxides⁴⁾ and spinel-type oxides^{5–7)} have been investigated as catalysts for this reaction.

It was reported that V₂O₅ was the most active transition metal oxide for the catalytic oxidation of soot⁸⁾ and its activity was further enhanced when promoted with CuO and/or K₂O.^{9,10)} For the simultaneous NO_x-soot removal, on the other hand, K-promoted CuO (K/CuO) was reported to be superior to K/V₂O₅ with respect to either soot oxidation or NO reduction.¹⁾ Referencing to these results and aiming at the stabilization of K in a mixed oxide crystal lattice, we designed an oxide catalyst having an overall metal composition of La/K/Cu/V = 9/1/7/3 (denoted as LKCVO) as a catalyst for the simultaneous NO_x-soot removal.³⁾

The LKCVO oxide was originally designed to form a perovskite-type oxide (ABO₃) with La and K at A position and Cu and V at B position. It is well known that the geometric condition and charge neutrality should be satisfied for a given combination of A- and B-site cations to crystallize in the perovskite structure. It is generally required that ionic radii of A-site cations coordinated by twelve oxide ions, r_A , are larger than 0.9 Å and those of B-site cations coordinated by six oxide ions, r_B , are larger than 0.5 Å and usually smaller than 1.0 Å. In addition, the tolerance factor, $t = (r_A + r_O)/\sqrt{2}(r_B + r_O)$, should be between 0.75 and 1.0 to

form the perovskite-type structure. If each metal cation is assumed to have the most stable oxidation number and the ionic radii reported by Shannon¹¹⁾ are used (La³⁺; 1.36 Å, K⁺; 1.64 Å, Cu²⁺; 0.73 Å, V⁵⁺; 0.54 Å, O²⁻; 1.40 Å), the combination and composition of LKCVO satisfy geometrically required conditions, as shown below.

$$\begin{aligned} r_A^{\text{av}} &= 0.9r(\text{La}^{3+}) + 0.1r(\text{K}^{+}) = 1.388 \text{ Å}, \\ r_B^{\text{av}} &= 0.7r(\text{Cu}^{2+}) + 0.3r(\text{V}^{5+}) = 0.673 \text{ Å}, \\ t &= (r_A^{\text{av}} + r_O)/\sqrt{2}(r_B^{\text{av}} + r_O) = 0.95. \end{aligned}$$

If the LKCVO oxide crystallized in perovskite-type structure, it should have an oxygen deficient composition (La_{0.9}K_{0.1}Cu_{0.7}V_{0.3}O_{2.85}). In the actual result, however, LKCVO was not a single-phase perovskite but a mixture of several crystalline phases.³⁾ In spite of that, LKCVO was superior to other perovskite-type oxides with respect to the selectivity to NO_x reduction into N₂ in the simultaneous NO_x-soot removal.³⁾

As reported in this paper, the real active phase in LKCVO is (La_{2-x}K_x)(Cu_{0.95}V_{0.05})O₄ with 0.05 ≤ x ≤ 0.1, and we already reported⁴⁾ their catalytic properties in the simultaneous removal of NO_x and soot. This paper reports how we extracted the real active phase of (La_{2-x}K_x)(Cu_{0.95}V_{0.05})O₄ from a mixture of several phases. We took the following approach. Crystalline phases present in the LKCVO mixture were identified by X-ray diffraction (XRD) and energy dispersive spectroscopy (EDS) in a transmission electron microscope (TEM). And the catalytic activities of single-phase oxides, which were synthesized according to the results of XRD and TEM/EDS analyses, were compared with the cat-

alytic activity of LKCVO. The present results prove the usefulness of the combined use of XRD, TEM/EDS and the activity measurement in extracting the real active phase from the mixture.

Experimental

Materials. Mixed metal oxides were prepared from p.a. grade La(CH₃COO)₃·1.5H₂O, K(CH₃COO)·H₂O, Cu(CH₃COO)₂·H₂O, and NH₄VO₃. An appropriate mixture of starting chemicals was put into deionized water. Although NH₄VO₃ was not completely dissolved in water and it decomposed into V₂O₅ upon heating, the suspension solution was forced to evaporate to dryness under vigorous stirring. The resulting solid precursor was well ground and then calcined in air at 850 °C for 5–10 h (LKCVO and K₂NiF₄-type oxides) or at 1000 °C for 10 h (LaVO₄ and La₃VO₇). CuO was commercially obtained and subjected to the catalytic test as received.

Characterization. Powder X-ray diffraction (XRD) patterns were recorded on a RINT2000 diffractometer (Rigaku) using Cu Kα radiation. The LKCVO sample was ground in butyl alcohol and then dispersed on a holey carbon film supported on an Ni grid, and analyzed in a transmission electron microscope (TEM; JEOL 2000FX) equipped with an energy dispersive spectrometer (EDS; LINK AN 10000). The metal content of individual crystallites was determined by spot analysis with the electron beam focused to 20–30 nm in diameter.

Catalytic Activity Measurement. Catalytic activity for the simultaneous removal of NO_x and Diesel soot particulate was measured by the temperature programmed reaction method.^{3–7)} The Diesel soot particulate, in which the soluble organic fraction was less than 5% in weight, was obtained by the incomplete combustion of Diesel fuel. The catalyst and soot (ca. 5 wt%) were well mixed by grinding for 10 min in an agate mortar, then the mixture was pelletized under the pressure of 400 kg cm⁻², crushed, and sieved to 20–60 mesh. The catalyst/soot mixture (0.33 g) was placed in a quartz-tube reactor and, after pretreatment at 400 °C for 3 h and cooling down to 100 °C in a helium stream, the catalyst bed was heated at a rate of 1 °C min⁻¹ in a gaseous mixture of NO (0.5%), O₂ (5%), and He (balance) flowing at 20 cm³ min⁻¹. The outlet gas was analyzed at intervals of about 15 min by a TCD gas chromatograph (Shimadzu GC-8A) with a Molecular Sieve 5A column for separating O₂, N₂, NO, and CO and a Porapak Q column for CO₂ and N₂O.

It has been reported that the simultaneous NO_x-soot removal

reaction takes place at the three-phase region where the solid catalyst, the solid soot and the gaseous reactants (NO_x, O₂) meet together^{2–4)} and that the contact between the catalyst and the soot significantly influences the catalytic performance.^{12,13)} We confirmed separately^{2,4)} that the mixing procedure used in this study gave the tight catalyst/soot contact with which the catalytic activity was the highest and no longer influenced by the prolonging mixing. Under that condition, the catalytic performance was little influenced by the specific surface area of the catalyst.²⁾

Results and Discussion

Crystalline Phase Analysis by XRD. Figure 1 shows the XRD pattern of the LKCVO sample. By making reference to JCPDS data and elemental analysis (see below), LKCVO was proven to be composed of CuO and three La-containing mixed metal oxides analogous to La₂CuO₄, LaVO₄, and La₃VO₇. XRD peaks from CuO and the LaVO₄ analogue were almost consistent with the reported ones,¹⁴⁾ while those from the other two phases slightly shifted toward larger 2θ direction as compared with pure La₂CuO₄¹⁵⁾ and La₃VO₇.¹⁶⁾

Elemental Analysis of Grains by TEM/EDS. Metal compositions of grains present in LKCVO were analyzed by TEM/EDS. There were no grains having the weighted-in composition. Except for Cu-rich grains, almost all the analyzed grains contained La as a major component in ca. 50–70 atom%, indicating the formation of La-containing mixed metal oxides. Figure 2 shows the metal compositions of the La-containing grains, where the compositions of K, Cu, and V are plotted against the La composition for each grain. Although the observed compositions were somewhat scattered, they can be reasonably categorized into the following three groups according to the compositional ratio of two metal cations in larger quantities: a) La/V ≈ 1; La (51–54%), V (43–48%), b) La/Cu ≈ 2; La (65–69%), Cu (26–32%), c) La/V ≈ 3; La (64–71%), V (22–26%). The average compositions of the La/V ≈ 1, La/Cu ≈ 2, and La/V ≈ 3 phases are summarized in Fig. 3. These three phases certainly correspond respectively to LaVO₄, La₂CuO₄, and La₃VO₇ analogues suggested by XRD. As stated above, XRD peaks of the La/Cu ≈ 2 and La/V ≈ 3 phases in the LKCVO mixture slightly shifted from those of pure La₂CuO₄¹⁵⁾ and

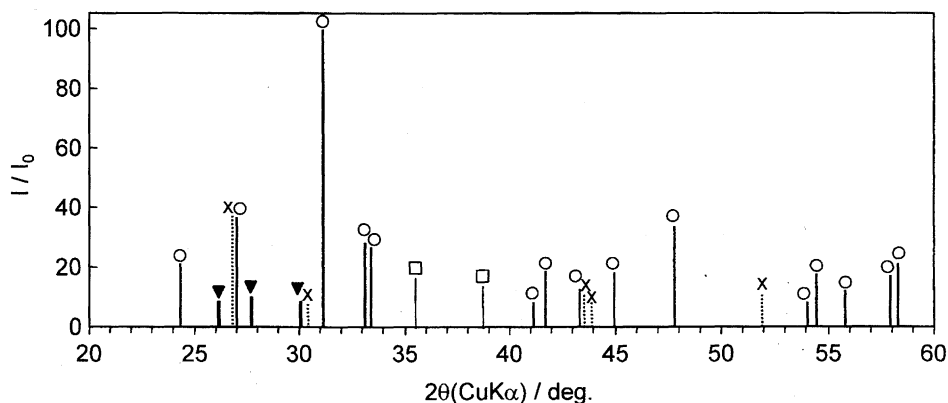


Fig. 1. Powder X-ray diffraction pattern of LKCVO having an overall metal composition of La/K/Cu/V = 9/1/7/3. O; La₂CuO₄-analogue phase, □; CuO, ▼; LaVO₄-analogue phase, ×; La₃VO₇-analogue phase.

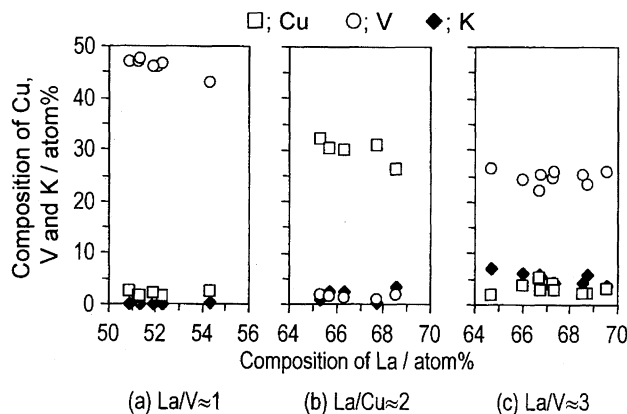


Fig. 2. Metal compositions of grains present in LKCVO detected by TEM/EDS.

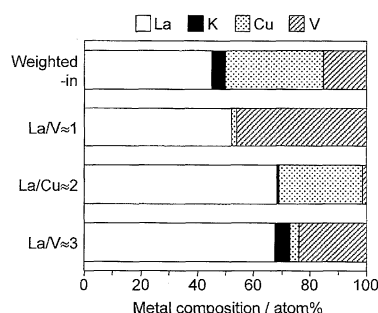


Fig. 3. Average metal composition of phases found in LKCVO.

La_3VO_7 ,¹⁶⁾ respectively. This indicates that minor components, K and V in the $\text{La}/\text{Cu} \approx 2$ phase and K and Cu in the $\text{La}/\text{V} \approx 3$ phase, are present in the structures to form solid solution phases. On the other hand, almost identical XRD patterns of the $\text{La}/\text{V} \approx 1$ phase and pure LaVO_4 suggest that Cu detected as a minor component is present not in the bulk of the mixed oxide but most probably on the surface of LaVO_4 .

As can be seen from Fig. 1, the La_2CuO_4 analogue is the main crystalline phase present in LKCVO. Its average metal composition is $\text{La}/\text{K}/\text{Cu}/\text{V} = 66.7/2.0/29.8/1.5$ which yields a K_2NiF_4 -type composition of $(\text{La}_{1.94}\text{K}_{0.06})(\text{Cu}_{0.95}\text{V}_{0.05})\text{O}_4$. It should be noted that the observed Cu/V ratio (0.95/0.05) is fairly in accordance with the reported solubility limit of V in $(\text{La}_{1.85}\text{Sr}_{0.15})(\text{Cu}_{1-x}\text{V}_x)\text{O}_{4-\delta}$.¹⁷⁾

Temperature Programmed Reaction (TPR) of the Simultaneous NO_x -Soot Removal. Figure 4 shows a TPR result of the simultaneous NO_x -soot removal with the LKCVO catalyst. When the soot/catalyst mixture was heated in the $\text{NO}-\text{O}_2$ reaction gas, the formation of CO_2 due to the oxidation of the soot increased, reached a maximum and suddenly dropped due to the exhaustion of the charged soot. The concurrence of the formation of CO_2 and the reduction of NO into N_2 indicates that the simultaneous NO_x -soot removal reaction proceeds.²⁻⁷⁾ When N_2 and CO_2 are only products as shown in Fig. 4, the overall reaction can be written as $\text{C} + (1-\alpha)\text{O}_2 + 2\alpha\text{NO} \rightarrow \alpha\text{N}_2 + \text{CO}_2$. Here, α refers to as a fraction of soot (C) reacted with NO to form N_2 ; the value of α was 0.06 for the LKCVO catalyst.

From the TPR results, two parameters are derived in or-

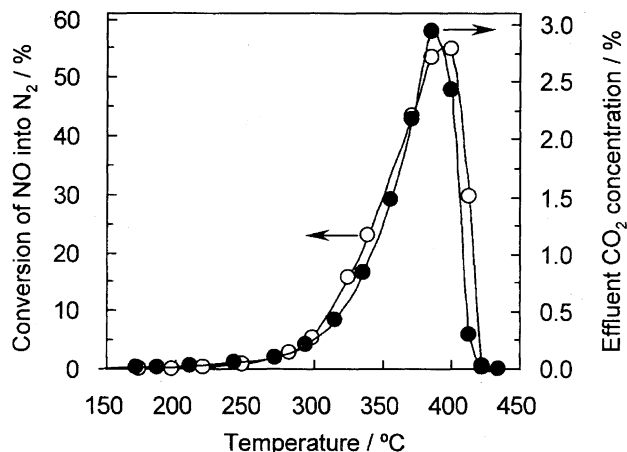


Fig. 4. Temperature programmed reaction of the simultaneous NO_x -soot removal over the LKCVO catalyst. Heating rate; 1°C min^{-1} . Gas composition; $\text{NO } 0.5\%$, $\text{O}_2 \text{ } 5\%$, balance He. Flow-rate; $20 \text{ cm}^3 \text{ min}^{-1}$.

der to compare the catalytic performance for the NO_x -soot removal. One is the ignition temperature of soot (T_{ig}), which is estimated by extrapolating the steeply ascending portion of the CO_2 formation curve to zero CO_2 concentration (estimated error, $\pm 5^\circ\text{C}$). The other is the total amount of N_2 formed throughout the TPR run ($V[\text{N}_2]$), which is obtained by integrating the conversion versus temperature (time) curve. As reported before,²⁻⁷⁾ T_{ig} and $V[\text{N}_2]$ can be used as measures of the catalytic activity and the selectivity to NO reduction, respectively.

Identification of the Real Active Phase by the Measurement of Catalytic Performance. The combined use of XRD, TEM, and EDS revealed that LKCVO was composed of CuO and mixed metal oxides analogous to La_2CuO_4 , LaVO_4 , and La_3VO_7 . In order to identify the real active phase, single-phase oxides suggested by XRD and TEM/EDS analyses were synthesized and their catalytic activities for the simultaneous NO_x -soot removal were measured. It can be speculated from the results of phase analysis that the predominant La_2CuO_4 analogue which contains a small amount of K and V might play a major role in catalysis. The catalytic performance was first compared for pure oxides, CuO , La_2CuO_4 , LaVO_4 , and La_3VO_7 , to establish the intrinsic catalytic properties of the respective phases.

Figure 5 shows N_2 formation curves obtained with pure oxide catalysts. As can be seen from Fig. 4, onsets of CO_2 and N_2 formation curves are very close to each other. Accordingly, the lower onset temperature of the N_2 formation curve indicates the higher activity of the catalyst. Since the amount of the charged soot was the same for all the catalyst/soot mixtures, the larger $V[\text{N}_2]$ means the larger value of α , that is, the higher selectivity to N_2 formation. CuO was the most active but less selective; La_2CuO_4 was the most selective and moderately active; and two vanadates, LaVO_4 and La_3VO_7 , were less active and selective. As can be seen from the $V[\text{N}_2]$ vs. T_{ig} plot (Fig. 6), the catalytic performance of La_2CuO_4 was the closest to LKCVO among the pure oxides, confirming the prospect that La_2CuO_4 will

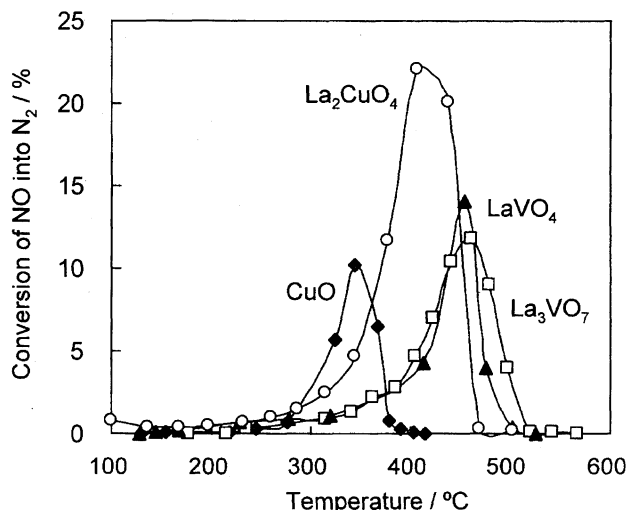


Fig. 5. Nitrogen formation curves during temperature programmed NO_x -soot removal reaction over CuO , La_2CuO_4 , LaVO_4 , and La_3VO_7 .

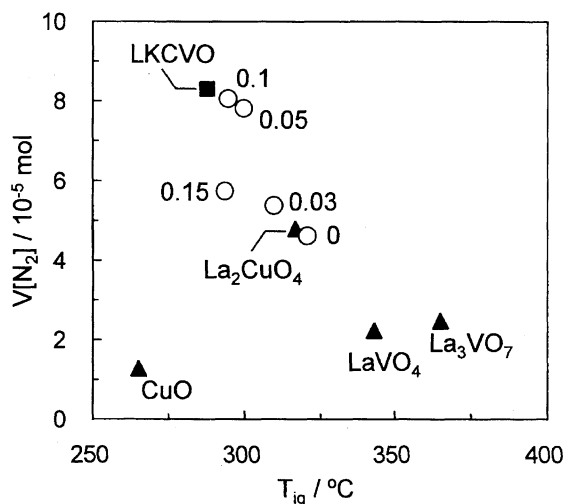


Fig. 6. Relation between the amount of N_2 formed throughout the TPR run ($V[\text{N}_2]$) and the ignition temperature of soot (T_{ig}) of oxides in La-K-Cu-V-O system. \circ ; $(\text{La}_{2-x}\text{K}_x)(\text{Cu}_{0.95}\text{V}_{0.05})\text{O}_4$ oxides are designated by numerical values of x .

be a suitable host material of the active phase.

To determine the composition of the real active phase, a series of K_2NiF_4 -type $(\text{La}_{2-x}\text{K}_x)(\text{Cu}_{0.95}\text{V}_{0.05})\text{O}_4$ oxides were synthesized and their catalytic performance for the NO_x -soot removal reaction was examined (Fig. 6); the V content was fixed at 0.05 with reference to the EDS analysis while the K content varied between 0 to 0.15. Almost the same catalytic performance of La_2CuO_4 and $\text{La}_2\text{Cu}_{0.95}\text{V}_{0.05}\text{O}_4$ indicates that the doping of a small amount of V influences the catalytic property very little. The content of K, on the other hand, caused a significant effect on the catalytic performance. With increasing the K content (x), both the activity and the selectivity progressively increased up to $x = 0.1$, and then the selectivity decreased at $x = 0.15$ with the activity being unchanged. Such a promotion effect and the

presence of the optimum substitution level of K were also observed in perovskite-type $\text{La}_{1-x}\text{K}_x\text{CoO}_3$ ^{2,3)} and spinel-type $\text{Cu}_{1-x}\text{K}_x\text{FeO}_4$.⁷⁾ We reported previously that the solubility limit of K in $(\text{La}_{2-x}\text{K}_x)(\text{Cu}_{0.95}\text{V}_{0.05})\text{O}_4$ was close to $x = 0.1$.³⁾ Accordingly, K dissolved in the crystal lattice functions well as a promoter, while beyond the solubility limit ($x = 0.15$), the excess K covers the surface active sites of the $(\text{La}_{2-x}\text{K}_x)(\text{Cu}_{0.95}\text{V}_{0.05})\text{O}_4$ mixed metal oxide and thus deteriorates the catalytic performance.

As can be seen from Fig. 6, oxides with $x = 0.05$ and 0.1 showed the catalytic performance comparable but slightly inferior to the LKCVO catalyst. The slight superiority of the LKCVO catalyst, which is a mixture of the main phase of $(\text{La}_{2-x}\text{K}_x)(\text{Cu}_{0.95}\text{V}_{0.05})\text{O}_4$ and minor phases of CuO and two vanadate analogues, might imply that the minor phases, most probably active CuO , synergistically contribute to the catalytic performance. Anyway, the results shown in Fig. 6 are sufficient to conclude that $(\text{La}_{2-x}\text{K}_x)(\text{Cu}_{0.95}\text{V}_{0.05})\text{O}_4$ with $x = 0.05$ –0.1 is the real active phase in LKCVO. The composition of K confirmed by the catalytic tests was consistent with that suggested by EDS ($x = 0.06$).

Cell Parameters. Single-phase $(\text{La}_{2-x}\text{K}_x)(\text{Cu}_{0.95}\text{V}_{0.05})\text{O}_4$ crystallized in the orthorhombic system. The following cell parameters were obtained for $x = 0.05$ and 0.1; $a = 5.324$, $b = 5.385$, $c = 13.114$ Å ($x = 0.05$) and $a = 5.344$, $b = 5.384$, $c = 13.101$ Å ($x = 0.1$). The K_2NiF_4 -type oxide present in LKCVO also had a orthorhombic unit cell with $a = 5.349$, $b = 5.390$, $c = 13.10$ Å. Making allowance for the interference of diffraction peaks from other crystalline phases in the LKCVO mixture, it may be said that the cell parameter of the K_2NiF_4 -type oxide in LKCVO is close to those of the single-phase oxides ($x = 0.05$ and 0.1). This also confirms that $(\text{La}_{2-x}\text{K}_x)(\text{Cu}_{0.95}\text{V}_{0.05})\text{O}_4$ with $x = 0.05$ –0.1 is the real active phase.

Conclusions

The phase analysis by XRD and TEM/EDS revealed that the oxide catalyst having an overall metal composition of $\text{La}/\text{K}/\text{Cu}/\text{V} = 9/1/7/3$ (LKCVO) consisted of CuO and three La-containing mixed oxides analogous to La_2CuO_4 , LaVO_4 , and La_3VO_7 . The predominant phase was the La_2CuO_4 analogue with an average composition of $\text{La}/\text{K}/\text{Cu}/\text{V} = 66.7/2.0/29.8/1.5$ or $(\text{La}_{1.94}\text{K}_{0.06})(\text{Cu}_{0.95}\text{V}_{0.05})\text{O}_4$. From the comparison of the catalytic performance of LKCVO with those of single-phase oxides synthesized according to the results of XRD and TEM/EDS, $(\text{La}_{2-x}\text{K}_x)(\text{Cu}_{0.95}\text{V}_{0.05})\text{O}_4$ with $0.05 \leq x \leq 0.1$ was identified to be the real active phase in LKCVO for the simultaneous NO_x -soot removal reaction.

The present results demonstrate that the combined use of XRD and TEM/EDS for phase analysis and the catalytic measurement is quite powerful to extract the real active phase from a mixture of several phases.

This study was partly supported by a Grant-in-Aid from the Ministry of Education, Science, Sports and Culture.

References

- 1) K. Yoshida, S. Makino, S. Sumiya, G. Muramatsu, and R. Helferich, *SAE Paper*, No. 892046 (1989).
 - 2) Y. Teraoka and S. Kagawa, "Catalysis Surveys from Japan," in press.
 - 3) Y. Teraoka, K. Nakano, S. Kagawa, and W. F. Shangguan, *Appl. Catal. B*, **5**, L181 (1995).
 - 4) Y. Teraoka, K. Nakano, S. Kagawa, and W. F. Shangguan, *Catal. Today*, **27**, 107 (1996).
 - 5) W. F. Shangguan, Y. Teraoka, and S. Kagawa, *Appl. Catal. B*, **8**, 217 (1996).
 - 6) W. F. Shangguan, Y. Teraoka, and S. Kagawa, *Appl. Catal. B*, **12**, 237 (1997).
 - 7) W. F. Shangguan, Y. Teraoka, and S. Kagawa, *Appl. Catal. B*, **16**, 149 (1998).
 - 8) A. F. Ahlström and C. U. I. Odenbrand, *Appl. Catal.*, **60**, 143 (1990).
 - 9) A. F. Ahlström and C. U. I. Odenbrand, *Appl. Catal.*, **60**, 157 (1990).
 - 10) P. Ciambelli, P. Corbo, P. Parrella, M. Scialò, and S. Vaccaro, *Thermochim. Acta*, **162**, 83 (1990).
 - 11) R. D. Shannon, *Acta Crystallogr., Sect. A*, **A32**, 751 (1976).
 - 12) J. P. A. Neeft, O. P. van Pruissen, M. Makkee, and J. A. Moulijn, *Appl. Catal. B*, **12**, 21 (1997).
 - 13) J. P. A. Neeft, M. Makkee, and J. A. Moulijn, *Appl. Catal. B*, **8**, 57 (1996).
 - 14) JCPDS 25-427 (LaVO_4) and 5-661 (CuO).
 - 15) JCPDS 30-487.
 - 16) JCPDS 37-894.
 - 17) J. B. Wallance, E. A. Payzant, H. W. King, G. Stoink, and D. C. Dahn, *J. Appl. Phys.*, **69**, 4857 (1991).
-